Metals' synergetic effect in a promising Ru^{II}-Pt^{II} assembly for a combined anticancer approach: Theoretical exploration of the photophysical properties

Marta E. Alberto,*[a] Nino Russo, [b] Carlo Adamo [a,c]

Abstract: Ru^{II}-Pt^{II} complexes are members of a novel and very interesting class of bioactive molecules of interest as anti-cancer agents, obtained combining a light-absorber chromophore with a cisplatin-like unit. The results of a carefully DFT and TDDFT investigation on a Ru^{II}-complex and its conjugate with *cis*$PtCl_2$-moiety reveal that a successful metals effect makes the assembly promising as multitarget anticancer drug. The inspection of Type I and Type II photoreactions and spin-orbit coupling computations reveal that *cis*-$PtCl_2$ moiety is able to improve the photophysical properties of the Ru^{II}-chromophore, ensuring an efficient $^1O_2$ generation and making the assembly suitable for PDT approach. At the same time, Ru^{II}-chromophore promotes a new alternative activation mechanism of Pt^{II} ligand via a ^{3}MLCT state, before reaching the biological target. The importance of the supramolecular architecture is herein accurately described opening new interesting perspectives on the use of bimetallic Ru^{II}-Pt^{II} assemblies in a combined anticancer approach.

Introduction

Photodynamic Therapy (PDT) is receiving an increasing attention worldwide as a less invasive medical treatment and due to its highly reliable tumour ablative ability. [1] The relative simplicity of this intervention together with the selective destruction of neoplastic tissue through direct cellular damage has let to worldwide acceptance and growth. As currently practiced, PDT employs a photosensitizer (PS) which upon irradiation, triggers a sequence of photochemical and photobiological processes leading to tumour cells necrosis and/or apoptosis by producing the highly cytotoxic singlet oxygen ($^1O_2$).

The photochemical processes involved in PDT starts with the excitation of the PS from its ground S_0 to the excited S_1 state, followed by non-radiative intersystem spin crossing (ISC) mechanism from S_1 to the triplet state T_1. Quenching mechanisms of T_1 state can generate two different classes of reactions, called Type I and Type II photoreactions. [2]

Type II photoreactions arise from direct energy transfer between the chromophore in its excited triplet state (^{3}Ps*) and ground-state molecular oxygen ($^3O_2$) to yield chemically highly active singlet oxygen $^1O_2$. The latter is able to react with many biological molecules, including lipids, proteins, and nucleic acids leading to cancer cell death and representing, accordingly, the putative cytotoxic agent in PDT.

On the other hand, Type-I photoreactions originate from electron exchange reactions between the excited ^{3}Ps* and organic substrates, producing radical intermediates that are subsequently scavenged by oxygen, with the formation of the superoxide oxygen radical species $O_2^{\cdot(-)}$ and other highly reactive radicals.

To some extent, the T_1 deactivating pathways are in competition among them and, to cause irreversible destruction of tumour cells, type II should predominate over the other, in that singlet oxygen shows relatively high reactive property.

To generate type II reactions, a successful PS should possess: *i)* a red-shifted absorption wavelength, falling in the so-called therapeutic window ($500<\lambda<800$ nm), to deeply penetrate human tissues; *(ii)* a singlet–triplet energy gap (ΔE_{S-T}) higher than the energy required to generate the singlet oxygen (0.98 eV); *(iii)* a consistent spin–orbit coupling from the excited S_1 to T_n electronic states to ensure an efficient ISC mechanism, that in turn, increases the production of singlet oxygen.[2]

To further advance the novel PDT treatment, the design, synthesis and characterisation of new PSs with improved efficiency and side effect profiles is needed, together with a more thorough and integrated understanding of the multitude of targets/actions so far ascribed to PDT.

In the last years, the search for new active sensitizers has been substantially diversified by testing several types of dyes, introducing heavy substituents and various transition metals in the macrocycles, in the attempt to move away from the traditional porphyrin-as-PS paradigm. The aim is to modulate the chemical, photophysical and biological properties of these molecules so that they could appear successful therapeutic agents. [2]

One of the newest and most challenging one, still in its infancy, is to functionalize a PS with a *cis*platin-like compound. [3] These kinds of conjugates are likely to increase the lethality of PDT treatment. Significant scientific works recently appeared and some compounds have been already proposed. [3]

The hypothesis for the use of such systems is based not only on the combined effect of PDT and cytostatic activity, but also on a

[a] Dr. M.E. Alberto, Prof. Dr. C. Adamo,
Institut de Recherche de Chimie Paris (IRCP), Chimie ParisTech, PSL Research University, CNRS, 11 P. et M. Curie, F-75005, Paris, France
E-mail: marta.alberto@chimie-paristech.fr
[b] Prof. N. Russo
Dipartimento di Chimica e Tecnologie Chimiche, Università della Calabria, via P. Bucci, 87036 Arcavacata di Rende (CS), Italy
[c] Prof. Dr. C. Adamo
Institut Universitaire de France, 103 Boulevard Saint Michel, F-75005 Paris, France

Supporting information for this article is given via a link at the end of the document.

better distribution Pt-mediated of the PS within the tumour and on the addressing of the drawbacks associated with the classical Pt-chemotherapy. [3]

Ru^{II}-Pt^{II} conjugates complexes are promising in this field. [4] They are multifunctional, forming coordinate covalent bonds to DNA through their *cis*-$PtCl_2$ moiety and photocleaving DNA through their Ru polypyridine chromophores. [5] While the ability of Ru^{II}-Pt^{II} heteronuclear complexes to bind DNA has been recently demonstrated, [4-5] their mechanisms of action have not yet been reported. Moreover, the effect of *cis*-$PtCl_2$ moiety on the photophysical properties related to their use as PDT agents, have not yet been investigated.

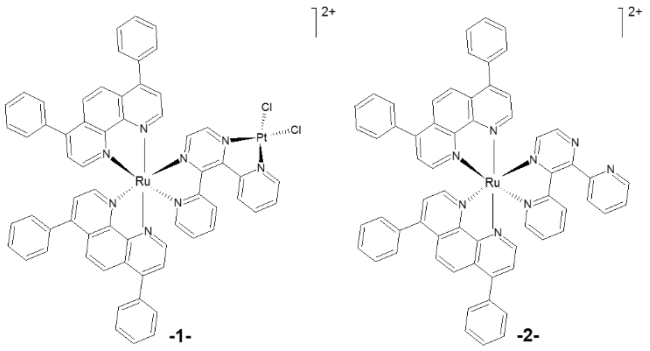

Scheme1: Ru-complex **-1-** and Ru^{II}-Pt^{II} assembly **-2-**, herein investigated

Herein, we report a careful DFT and TDDFT investigation of the photophysical properties of $[(Ph_2phen)_2Ru(dpp)]^{2+}$ **-1-** and of the new promising conjugate $[(Ph_2phen)_2Ru(dpp)PtCl_2]^{2+}$ **-2-** (Scheme1), recently synthesized. [5]

The influence of Pt^{II}-moiety on the crucial chemical and physical properties of the photosensitizer has been accurately described investigating Type I and Type II photoreactions, also including the magnitude of spin orbit coupling (SOC). On the other hand, the effect of Ru^{II}-chromophore on the activation mechanism of *cis*-$PtCl_2$ unit has been evaluated analysing the possible chloride ligand substitution mechanisms that can take place before reaching its biological target. Indeed, it is generally accepted that the early steps of triggering cell death by cisplatin-like compounds involve the loss of one or both chloride ligands leading to the formation of charged active species for subsequent interaction with DNA and other cellular nucleophiles. [6]

Our results show that *cis*-$PtCl_2$ moiety successfully modulate important properties of the Ru-chromophore enhancing its potential in PDT approach and opening new interesting perspectives on the use of the bimetallic Pt^{II}-Ru^{II} assembly as photosensitizer for PDT. Moreover, the access to the ^{3}MLCT triplet state promoted by a successful cooperative metals effect, allows for an alternative activation mechanism of Pt^{II} ligand before reaching DNA, *via* a low energy light induced photolabilization process.

Results and Discussion

UV-Vis Absorption Spectra: In order to evaluate the effect of cis-$Pt^{II}Cl_2$ moiety on the photophysical properties of Ru^{II}-chromophore, the electronic absorption spectra of molecules -**1-** and -**2-** have been computed in water and fully characterized. The superimposition of the spectra is depicted in Figure 1.

Main singlet electronic energies, molecular orbital (MOs) plots and more detailed information are reported in the Supporting Information (SI).

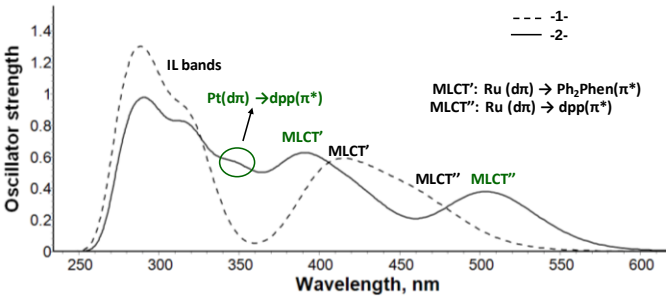

Figure1: Computed Absorption Spectra of **-1-** and **-2-**, in water, at the M06/6-31G(d,p)/SDD level of theory

Both complexes are efficient light absorbers throughout the UV and visible regions. As it can be observed in Figure 1, the introduction of cis-Pt moiety produces a significant effect on the absorption spectrum that falls in the visible region leaving almost unchanged the UV one.

Actually, the lowest UV region of the spectrum of both molecules, is characterized by a strong intense band around 290 nm and a less intense one around 320 nm. According to our analysis, in the case of the monometallic complex **-1-**, the first band originate from strong Ph_2Phen intraligand (IL) π→π* transitions, centred around 287 nm (See SI) in very good agreement with the available experimental value (274nm). [5] The molecular orbitals involved in such transitions (see SI) clearly indicate and confirm the **IL** nature of the band, as experimentally suggested, being unequivocally localized on the Ph_2Phen ligand.

In the same region, the Ru complex **-1-** shows another **IL** transition, computed at 298 nm (vs 310 nm exp) whose unequivocally dpp-based nature is revealed by the involved orbitals localized on the ligand, reported in the SI section. The same band for complex **-2-**, is composed only by Ph_2Phen intraligand (IL) π→π* transitions. No dpp-based IL transition has been found at such wavelengths. The second band observed in both spectra, originate by two transitions of comparable intensity computed at 317 and 318 nm for both **-1-** and **-2-** complexes. On the basis of the involved orbitals, such transitions have been assigned to a Ph_2Phen-based π→π* transitions. To further confirm our characterization, we computed also UV-Vis spectrum of the single Ph_2Phen ligand confirming the presence of the IL band at the same wavelengths (see ESI). The second band was, instead, previously assigned as a dpp-based IL. [5] On the contrary, our calculations show that the dpp-based transition in the case of complex **-2-,** experiences a hypsochromic shift at 346 nm, as effect of the platination process. The MO composition of such a

quite strong band, reveals a contribution of the dpp-based π→π* transition, mixed at Pt→dpp CT one.

Our evidences have been supported by the computed spectra of the single dpp ligand and Pt-dpp adduct, which confirm not only the hypsochromic shift of the dpp IL band upon platination but also the clear presence of a Pt→dpp CT excitation in the same region. (See ESI) Accordingly, this band appears only in the Ru-Pt assembly **-2-** but it is missing in the spectrum of the monometallic complex **-1-**. It is worth of note that no assignment for this band was previously done, although it was experimentally detected. [5]

The visible region of the spectrum, the most interesting for the PDT applications, is dominated by metal-to-ligand charge transfer (MLCT) transitions for each acceptor ligand.

For both compounds **-1-** and **-2-**, the Ru(dπ)→Ph_2Phen(π*) CT bands (**MLCT'** in Figure 1), result to be composed by three transitions (centred around 429 and 413 nm, for **-1-** and **-2-**, respectively, see ESI for more details), whose orbital composition unambiguously support the MLCT nature of the band, experimentally located at 424 nm.

The second MLCT band, characterized as a Ru(dπ)→dpp(π*) CT one, has been computed at 471 nm for Ru complex **-1-** (**MLCT''** in Figure 1), against the experimental value of 474 nm. Its nature is demonstrated by the localization of the involved orbitals on the Ru metal and on the dpp ligand. Upon platination, such band experiences a shift to 508 nm, as also experimentally found. The MLCT'' band is generated by a transition from the Ru(dπ)-HOMO-2 to dpp(π*)-based LUMO, for the monometallic complex **-1-** while involves Ru(dπ)-based HOMO, HOMO-1 and HOMO-2 orbitals to dpp(π*)-based LUMO and dpp(π*)-based LUMO+1 ones, in the case of bimetallic conjugate **-2-**. The red shift of the λmax transition in the case of bimetallic assembly **-2-**, is a direct consequence of the stabilization of the dpp(π*) acceptor orbitals obtained upon platination, as shown in the MOs energetic diagram which also include HOMO and LUMO orbitals snapshots (Figure2).

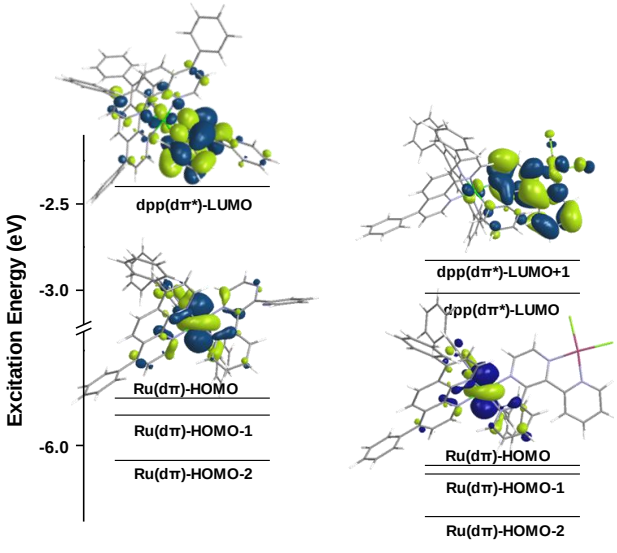

Figure 2: Relative energy (eV) and plot of Ru(dπ)-based occupied orbitals and dpp(π*)-based unoccupied ones, for molecules **-1-** and **-2-**

All the other involved orbitals are reported in the SI section. The hypsochromic shift of this band is of great interest for the application of such compound in PDT, since it can better penetrate human tissues, and represent, hence, one strategy to overcome the drawbacks of Ru^{II} compounds which generally require very high-energy light for the excitation.

Type II and Type I photoreactions: To promote Type II photoreactions, a good photosensitizer must be able to generate the cytotoxic singlet oxygen species promoting the O_2 $^3\Sigma_g^- \rightarrow {}^1\Delta_g$ transition by energy transfer. The amount of energy required to excite the molecular oxygen has been computed to be 0.90 eV, [7a] in good agreement with the experimental value of 0.98 eV. As a consequence, to achieve a good singlet oxygen quantum yield, the PS must possess a singlet-triplet energy gap (Δ_{S-T}) larger than that of O_2 to permit the energy transfer process to take place. The energy diagram for the lowest S_n and T_n vertical excitation states (Figure 3) shows that both compounds could promote the formation of singlet oxygen, being the Δ_{S-T} of both compounds, higher than the energy required to promote the O_2 $^3\Sigma_g^- \rightarrow {}^1\Delta_g$ transition.

Obviously, an efficient triplet state population by ISC mechanism from the S_1 state is an indispensable requirement. Interestingly, two triplet states lie below S_1 for both **-1-** and **-2**, (T_1 and T_2), and one more triplet state is very close in energy (T_3), suggesting that the internal conversion from the higher triplet states can contribute to the deactivation pathway to populate the T_1 state. To establish the feasibility of the intersystem crossing, spin orbit coupling values (SOC) between S_1 and S_2 with the triplet states have been computed and reported in Figure 3.

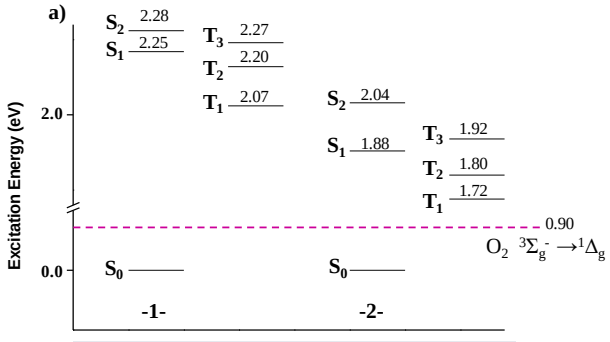

b)

SOC (cm^{-1})*	-1-	-2-
S_1-T_1	3.5	19.8
S_1-T_2	8.0	9.5
S_1-T_3	7.0	24.2
S_2-T_2	4.7	6.6
S_2-T_3	4.1	10.6

Figure 3. a) Vertical lowest singlet and triplet excitation energies (eV) for **-1-, -2-** and **O_2** at the M06/6-31G(d,p) level of theory; b) Computed S_1-T_1, S_1-T_2, S_1-T_3, S_2-T_2, S_2-T_3 SOC values (cm^{-1})

If compared with previous data reported for approved or potential PDT agents, [7] the SOC values suggest that the ^{3}MLCT state can be efficiently populated in both cases and can undergo Type II photoreactions producing the cytotoxic species $^1O_2$. Anyway, computations show that the presence of platinum in the assembly

-2-, significantly improves the ISC, thus suggesting a more efficient ^{3}MLCT state population. Actually, the S_1-T_1 SOC value computed for the assembly **-2-** is almost 6 times larger than that obtained for the monometallic complex **-1-**, and also the higher triplet states can be efficiently populated in the case of the bimetallic conjugate.

Our computations reveal that, besides improving the optical properties of the chromophore, the presence of platinum is able to promote the mixing of pure electronic states of different spin multiplicity increasing the rate of the intersystem spin crossing between S_1 and T_1 through the so-called heavy atom effect. A consequent increased production of singlet oxygen is thus expected.

The populated excited triplet state could also follow a different deactivation pathway photogenerating the superoxide anion $O_2^{\cdot-}$ and ROS through *Type II or TypeI reactions*, instead of transfer its energy to produce the singlet oxygen species. The feasibility of such kinds of photoreactions, can be established computing the vertical electron affinity (VEA) and ionization potentials (VIP) for each molecule and molecular oxygen. [8] Results are reported in Table1.

	VEA	VIP	*VEA(T_1)*	*VIP (T_1)*
-1-	-3.16	5.81	-5.39	3.48
-2-	-3.77	6.06	-5.63	4.20
$^3O_2$	-3.20	9.86		

Table 1: VEA and VIP values (eV) in water, for $^3O_2$ molecule and for **-1-** and **-2**- singlet and triplet excited states

The first $O_2^{\cdot(-)}$ generation pathways can be still included in type II-reactions since involves a direct electron transfer from the PS to O_2, according to reaction *(I)*

$$PS(T_1)+{}^3O_2 \rightarrow Ps^{\cdot(+)} + O^{\cdot(-)} \qquad (I)$$

Such reaction results to be not feasible in both cases, since the sum of VIP(T_1) of **-1-** or **-2-** and the electron affinity of $^3O_2$, is positive. Nevertheless, while for Ru complex **-1-** the process is not completely unreasonable in the triplet state, due to the small obtained positive value (+0.28eV), Ru^{II}-Pt^{II} assembly **-2-** instead, possesses much weaker electron-donating potential than -**1-** in water and the occurrence of such process can be ruled out.

The second pathway to generate $O_2^{\cdot(-)}$ may proceed through electron transfer from the reduced PS to molecular oxygen *(II):*

$$Ps^{\cdot(-)} + {}^3O_2 \rightarrow {}^1Ps + O_2^{\cdot(-)} \qquad (II)$$

The $Ps^{\cdot(-)}$ species could be formed in solution in presence of electron donors in the near vicinity e.g. a DNA base, or through the so-called autoionization reactions *(III* and *IV)* which imply the reduction of T_1 state of Ps by neighboring S_0 or T_1 state of Ps itself (Type-I photoreactions):

$$Ps\ (T_1) + Ps(S_0) \rightarrow Ps^{\cdot(+)} + Ps^{\cdot(-)} \qquad (III)$$
$$Ps\ (T_1) + Ps(T_1) \rightarrow Ps^{\cdot(+)} + Ps^{\cdot(-)} \qquad (IV)$$

According to our results, the T_1 states of both compounds can be reduced through autoionization reactions by neighboring T_1 ones, the sum of VEA (T_1) and VIP (T_1) being negative. The triplet state of **-2-** can be also reduced by a guanine base of DNA, for which a VIP of 5.49 eV has been previously computed at the same level of theory. [8] Nevertheless, from the data reported in Table 1, only the reduced triplet state of Ru-complex **-1-** can transfer an electron to the molecular oxygen in its ground state through reaction *(II)*, as confirmed by the higher electron affinity of oxygen compared to **-1-**. The superoxide anion can then undergo fast bimolecular decay to yield oxidising species as H_2O_2 and $OH^{\cdot}$, or acting itself as reducing agent for other Ru-compounds **-1-** in the triplet state. The same reaction results to be not-feasible in water for Ru^{II}-Pt^{II} **-2-** assembly. As a consequence, while monometallic complex **-1-** can undergo *Type I photoreactions* ultimately leading to production of $O_2^{\cdot(-)}$ and ROS, Ru^{II}-Pt^{II} assembly is able to promote only *Type II* ones leading to the singlet oxygen production. In view of the competition of the two deactivating pathways of triplet state and the possibility of electron transfer from the reduced triplet state of Ru-**1-** to molecular oxygen, the cytotoxic $^1O_2$ generation could be, in that case, limited.

For Ru^{II}-Pt^{II} conjugate **-2-,** only the direct energy transfer pathway to generate $^1O_2$ is energetically feasible and predominates over the other deactivation pathways of the ^{3}MLCT, which lead us to hypothesize, at least in water, a $^1O_2$ -yield higher than that displayed by monometallic Ru complex.

Pt^{II} Activation Mechanism. The Pt^{II} bioctive site coupled to the Ru^{II}-chromophore was previously found to ensure covalent binding of the mixed metal assembly to DNA.[5] Nevertheless, the activation mechanism of $Pt^{II}Cl_2$ before reaching the biological target in the supramolecular complex **-2-** is not known, although it was hypothesized its ability to photobind DNA via MLCT excitation.[5] Our results show that, upon irradiation, an efficient ISC process promoted by the assembly **-2-,** is able to warrant the population of the T_1 state, whether directly from S_1 or by internal conversion from the higher triplet states T_2 and T_3. Compared to the ground state, T_1 state is characterized by an enhanced electron density on dpp ligand, which lead to a reduction of Lewis acidity of platinum centre with a consequent higher polarization of the Pt-Cl bonds. The analysis of difference density plots between S_0 and both T_1 and T_2 excited states (showed in Figure 4), clearly show the direction of electron transfer toward the dpp ligand.

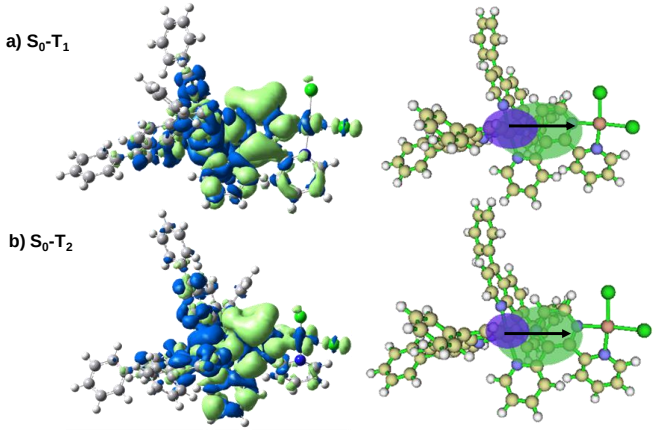

Figure 4: Electron Density Differences Plots between S_0-T_1 and S_0-T_2, for Ru^{II}-Pt^{II} assembly **-2-**

Natural Bond Orbital charges analysis (NBO) confirm the increased negative charge on dpp-$PtCl_2$ fragment in the T_1 state after excitation and a more positive charge on the Ru metal (see SI).

To explore the reactivity of the supramolecular Ru^{II}-Pt^{II} assembly **-2-** after irradiation, the Pt–Cl bond elongation process has been investigated along the T_1 and the lowest six excited states. The potential energy profiles are reported in Figure 5. They clearly show that a photolabilization of such bonds could be realized in the excited states. The very small energy barriers along the excited curves (less than 0.5 eV) support an easier release of the leaving group upon excitation, also confirming the occurrence of several state crossing between the excited singlet and triplet states. The proposed mechanism represents a unique example of a low energy light induced photolabilization of the Pt-Cl bond promoted by a ^{3}MLCT state accessible by ISC upon irradiation.

The promoted release of such ligands is expected to facilitate DNA binding and then represents an alternative way of activation of Pt^{II} compounds, in contrast to classical hydrolysis mechanism. [6,9-12]

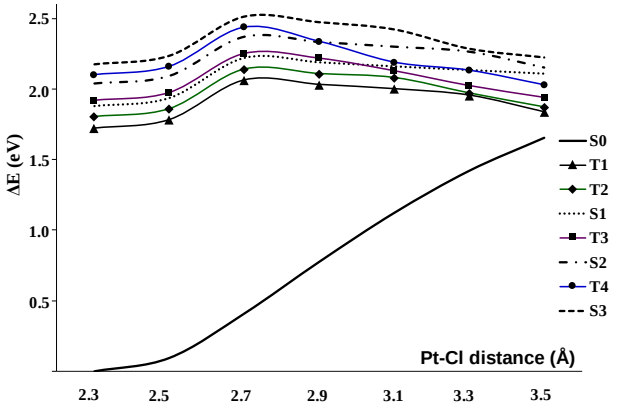

Figure 5. Potential energy profiles along the Pt–Cl coordinate of complex **-2-,** in its ground and lowest seven excited states

Actually, from the inspection of the first and second hydrolysis process in dark (Scheme 1), it results that the presence of Ru^{II}-chromophore bound to Pt^{II} moiety does not significantly modify the ligand-exchange kinetics compared with *cis*platin. This result is not surprising since it is now generally accepted that differences in the hydrolysis rates of Pt^{II}-compounds compared to cisplatin are correlated to the substitution of chlorides with bulkier leaving group. The modification of the spectator ammine groups instead, are thought to underlie differences in the biological activity connected with steric and chemical properties of DNA lesions. [6]

The optimized structures along the reaction path are reported in the SI section. Each step of the reaction proceeds *via* an associative mechanism through a penta-coordinated trigonal bipyramid transition state, in agreement with the hydrolysis mechanism displayed by anticancer Pt^{II} complexes, previously investigated. [9-12]

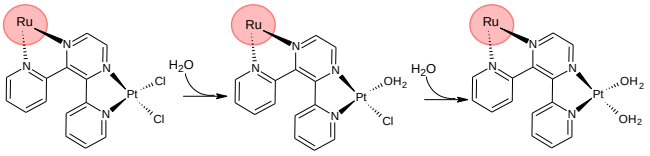

Scheme2: Investigated Hydrolysis Process for Ru^{II}-Pt^{II}conjugate **-2-**; *(Ru^{II}-polyazine ligands are omitted for clarity)*

According to our calculations, the first aquation reaction requires an energy barrier of 22.7 kcal/mol to be overcome, very similar to that previously computed for cisplatin.[11] The substitution of the second chloride requires a higher energy to occur, suggesting that also the assembly **-2-** could interact with DNA in its mono-hydrated form, as proposed for *cis*platin. Second and third-generation Pt^{II} drugs instead, are believed to reach the biological target in their fully hydrated form. Table 2 shows the activation energy values computed for cisplatin and for its analogues currently used in the medical protocols.

	Activation energies (kcal/mol)		
	First aquation	Second aquation	Rate limiting step
Ru^{II}-Pt^{II} -2-	**22.7**	**27.0**	second
Cisplatin [11]	22.9	26.2	second
Carboplatin [9a]	30.1	21.3	first
Nedaplatin [9b]	28.6	24.9	first
Oxaliplatin [9c]	27.9	24.1	first

Table 2: Computed activation energies (kcal/mol) for Ru^{II}-Pt^{II} **-2-** and cisplatin analogues

Our results hence provide a support of a DNA photobinding mechanism previously suggested, [5] giving evidences of a photolabilization process of Pt-Cl bond as an alternative activation mechanism of Pt^{II} moiety. The optical properties of Ru^{II}-chromophore are imparted onto the Pt-moiety enabling it to absorb wavelength otherwise inaccessible to Pt(II) compounds. These outcomes provide interesting insights on a low energy light induced release of chloride leaving group process.

The supramolecular architecture, thus, plays a crucial role in the Ru^{II}-Pt^{II} assembly **-2-,** promoting a successful synergetic effect between metals. *cis*-$Pt^{II}Cl_2$ moiety improves the optical properties of Ru^{II}-chromophore and enhances the spin-orbit coupling between singlet and triplet states of **-2-**, thus providing for a more efficient ISC between them and high expected $^1O_2$ production. Moreover, Pt coordination makes the ^{3}MLCT state able to selectively produce singlet oxygen through *Type II*-photoreaction, inferring, to the bimetallic complex, a too weak electron-donating potential to be involved in competitive electron transfer processes. At the same time, Ru^{II}-chromophore provides for a different activation mechanism of Pt^{II} compound, making easier the release of chloride ligands after excitation. The photolabilization of Pt-Cl bonds is a widely explored mechanism for Pt^{IV} compounds [13] but not for classical Pt^{II}

chemotherapeutic agent. Studies are under way to further explore this new possibility.

Conclusions

In summary, a detailed DFT and TDDFT study has been carried out on $[(Ph_2phen)_2Ru(dpp)]^{2+}$ **-1-** and on its promising assembly with cis-Pt^{II} moiety **-2-**. Results show that both monometallic complex **-1-** and heteronuclear Ru^{II}-Pt^{II} assembly **-2**, are able to generate, in aqueous environment, the cytotoxic singlet oxygen species $^1O_2$, having $\Delta_{S\text{-}T}$ gap higher enough to ensure the O_2 $^3\Sigma_g^- \rightarrow {}^1\Delta_g$ transition, combined with high SOC values. Interestingly, Ru^{II}-Pt^{II} complex **-2-** shows enhanced spin-orbit coupling values for all the considered channels, predicting a strong enhancement of the ISC process upon platination. The ^{3}MLCT excited triplet state of **-2-** is then more efficiently populated and could successfully promote *Type II photoreactions* leading to the cytotoxic singlet oxygen production. Moreover, inspection of *Type I* mechanisms reveals that the latter ^{3}MLCT state of **-2-** is exclusively involved in the $^1O_2$ generation, having a too weak e^- donating potential to be involved in the competitive electron transfer process to oxygen with production of superoxide anion. The not-feasibility of such process in water allow us to predict an efficient $^1O_2$ –yield. *Cis*platin unit makes then Ru^{II}-chromophore suitable for PDT applications, opening new interesting perspectives on the use of Ru^{II} as PSs.

On the other hand, the presence of the Ru^{II}-chromophore bound to $PtCl_2$ moiety promotes a possible alternative way of activation of Pt^{II} compounds before reaching its biological target, *via* a photorelease of the leaving group upon irradiation. The optical properties of Ru^{II}-chromophore are then imparted onto the Pt-moiety enabling it to absorb wavelengths otherwise inaccessible to Pt^{II} compounds and showing the importance of the supramolecular architecture.

We believe that these encouraging results will stimulate further investigations on bimetallic conjugates as new drugs for a combined treatment of cancer.

Experimental Section

All the calculations herein presented have been performed at DFT and its time-dependent TD-DFT formulation[14] by using the Gaussian 09 program code. [15] Ground state geometry optimizations have been performed in water without constrains by using the B3LYP exchange-correlation functional[16-17] in conjunction with the 6-31G(d,p) basis set for all atom except for Ru and Pt ones, which were described by the quasi-relativistic Stuttgart-Dresden pseudopotential.[18] Water environment has been simulated by means of the integral equation formalism polarizable continuum model (IEFPCM),[19] which corresponds to a linear response in non-equilibrium solvation. To confirm proper convergence to equilibrium and transition state geometries, vibrational frequency analysis has been carried out on the basis of analytical second derivatives of the Hamiltonian at this level of theory. To obtain more accurate activation energy barrier for the hydrolysis process of conjugate **-2-**, single-point calculations were also carried out with the larger basis set 6-31++G(2df,2pd).

Absorption spectra have been obtained in water, as vertical electronic excitations on the ground-state structures, employing M06[20] XC functional. The good performances of M06 in the reproduction of optical properties has been widely tested. [7,21]

Spin-orbit matrix elements have been computed using the quadratic-response TD-DFT approach[22-23] as implemented in the Dalton code, [24] at their ground state optimized geometries in the framework of the atomic-mean field approximation. [25] For this purpose, B3LYP coupled with the cc-pVDZ basis set for all the atoms has been used. The spin–orbit couplings (SOCs) have been defined according to the following formula:

$$SOC_{ij} = \sqrt{\sum_n \left|\langle \psi_{S_i} | \hat{H}_{SO} | \psi_{T_{j,n}} \rangle\right|^2}; \quad n = x, y, z$$

where $\hat{H}_{SO}$ is the spin–orbit Hamiltonian.

The Pt–Cl bond elongation on S_0 state has been studied performing a relaxed potential energy surface scan, with an increment of the coordinate of 0.2Å. Each single geometry was then employed for calculating 10 singlet and 10 triplet excited states by TD-DFT at the M06/6-31G(d,p)/SDD level of theory. The PEC along the Pt–Cl coordinate for the lowest 7 excited states are reported in the text. The zero-point of the energy scale is set to the ground-state energy at its equilibrium geometry.

Acknowledgements

This project has received funding from the European Union's Horizon 2020 research and innovation programme under the Marie Sklodowska-Curie grant agreement No 652999

Keywords: PDT • Singlet Oxygen • *cis*platin • anticancer drugs • Ru(II)complexes

[1] a) B.J. Quirk, G. Brandal, S. Donlon, J.C. Vera, T.S. Mang, A.B. Foy, S. M. Lewd, A.W. Girotti, S. Jogal, P.S. LaViolette, J.M. Connelly, H.T. Whelan *Photodiagnosis Photodyn Ther.* **2015**, *12*, 530-544; b) D.E.J.G.J. Dolmans, D. Fukumura, R.K. Jain, *Nature Rev. Cancer*, **2003**, *3*, 380-387; I.J. MacDonald, T.J. Dougherty *J Porphyr Phthalocyanines* **2001**, *5, 105-129.*

[2] a) S. Yano, S. Hirohara, M. Obata, Y. Haguya, S-I. Ogura, A. Ikeda, H. Kataoka, M. Tanaka, T. Joh J, *J. Photochem. Photobiol. C*, **2011**, *12*, 46-67 and references therein; b) A. P. Castano, P. Mroz and M. R. Hamblin, *Nat. Rev. Cancer*, **2006**, *6*, 535–545; c) A. P. Castano, T. N. Demidova, M.R. Hamblin, *Photodiagnosis and Photodyn Ther.* **2004**, *1*, 279-293; d) R. Padilla, J.A. Rodriguez-Corrales, L.E. Donohoe, B. S. J. Winkel, K.J. Brewer, *Chem. Commun*. **2016**, *52*, 2705-2708.

[3] a) A. Naik, R. Rubbiani, G. Gesser, B. Spingler, *Angew. Chem. Int. Ed.,* **2014**, *53*, 6938-6941; b) C. Lottner, K.C. Bart, G. Bernhardt, H. Brunner, *J Med Chem* 45, **2002**, 2079-2089; c) C. Lottner, K.C. Bart, G. Bernhardt, H. Brunner, *J Med Chem* **2002**, *45*, 2064-2078; d) M.F. Zuluaga, N. Lange N. *Curr Med Chem*, **2008**, *15*, 1655-1673;

[4] a) R. L. Williams, H.N. Toft, B. Winkel, K.J. Brewer, *Inorg. Chem.* **2003**, *42*, 4394-4400; b) M. Milkevitch, H. Storrie, E. Brauns, K.J. Brewer, B. W. Shirley, *Inorg. Chem*. **1997**, *36*, 4534–4538; c) R. Miao, M. T. Mongelli, D.F. Zigler, B. S. Winkel, K.J. Brewer, *Inorg. Chem.* **2006**, *45*, 10413–10415; d) A. Jain, B. Winkel, K.J. Brewer, *J. Inorg. Biochem.* **2007**, *101*, 1525-1528.

[5] a) S. L. H. Higgins, A.J. Tucker, B.S.J. Winkel, K.J. Brewer, *Chem. Commun*., **2012**, *48*, 67–69; b) S. L. H. Higgins, T.A. White, B.S J. Winkel, K.J. Brewer, *Inorg. Chem.* **2011**, *50*, 463–470;

[6] a) L. Kelland, *Nat Rev Cancer* **2007, 7,** 573-584; b) D. Wang, S. J. Lippard, *Nat. Rev. Drug Discovery*, **2005**, *4*, 307-320; c) Y. Jung, S. J. Lippard, *Chem. Rev.*, **2007**, *107*, 1387-1407; d) E. R Jamieson. S. Lippard, *J. Chem. ReV*. **1999**, *99*, 2467-2498; e) R.C Todd, S.J. Lippard, Metallomics, **2009**, *1*, 280–291

[7] a) M.E. Alberto, B.C. De Simone, G. Mazzone, E. Sicilia, N. Russo, Phys Chem Chem Phys **2015**, *17*, 23595-23601; b) M.E. Alberto, T. Marino, A. D. Quartarolo, N. Russo Phys.Chem.Chem. Phys. **2013,** *15,* 16167-16171; c) M. E. Alberto, B.C. De Simone, G. Mazzone, A.D. Quartarolo, N. Russo, *J Chem Theory Comput* **2014**, *10*, 4006−4013; d) M.E. Alberto, G. Mazzone, A.D. Quartarolo, F.F. Sousa, E. Sicilia, N. Russo, J Comput Chem **2014**, *35*, 2107–2113; e) M.E. Alberto, B.C. De Simone, G. Mazzone, T. Marino, N. Russo N. Dyes Pigm **2015**, *120*, 335-339;

[8] J. Llano, J. Raber, L.A. Eriksson, *J Photochem Photobiol A Chem.,* 154, 2003, 235-243

[9] a) M. Pavelka, M.F. Lucas, N. Russo, *Chem. Eur. J.* **2007**, 13, 10108 – 10116; b) M. E. Alberto, M.F. Lucas, M. Pavelka, N. Russo *J. Phys. Chem. B* **2009**, 113, 14473-14479; c) M. F. Lucas, M. Pavelka, M.E. Alberto, N. Russo, *J. Phys. Chem. B* **2009**, 113, 831-838; d) M.E. Alberto, V. Butera, N. Russo, *Inorg.Chem*. **2011**, 50, 6965-6971;

[10] Y. Zhang, Z. Guo, X-Z You *J. Am. Chem. Soc.* **2001,** *123,* 9378-9387;

[11] J. Raber, C. Zhu, L.A. Eriksson, *Mol. Phys*. **2004**, 102, 2537-2544

[12] M.E. Alberto, N. Russo, *Chem. Commun.* **2010***,* 47, 887-889

[13] a) L. Salassa, H. I. A. Phillips, P.J. Sadler, *Phys. Chem. Chem. Phys*., **2009**, *11*, 10311–10316; b) A.F. Westendorf, A. Bodtke, P.J. Bednarski Dalton Trans., **2011,** *40,* 5342-5351; c) Y. Zhao, J.A. Woods, N.J. Farrer, K.S. Robinson, J. Pracharova, J. Kasparkova, O. Novakova, H.Li, L. Salassa, A. M. Pizarro, G.J. Clarkson, L.Song, V. Brabec, P.J. Sadler *Chem. Eur. J.* **2013**, *19*, 9578 – 9591

[14] Casida M.E. In Recent Developments and Applications in Density-Functional Theory; J. M. Seminario, Eds.; Elsevier: Amsterdam, The Netherlands, **1996**, 155-192.

[15] Gaussian 09, Revision D.01, Gaussian, Inc., Wallingford CT, 2009 [The Complete Reference is reported in the SI section]

[16] A. D. Becke, *J. Chem. Phys*., **1993,** *98*, 5648–5652.

[17] C. Lee, W. Yang, R.G. Parr, *Phys. Rev. B*, **1988**, *37*, 785-789.

[18] D. Andrae, U. Haussermann, M. Dolg, H. Stoll, H. Preuss, *Theor. Chim. Acta* **1990**, *77***,** 123-141

[19] a) M. Cossi, V. Barone, *J Chem Phys* **2000**, *112*, 2427-35; b) J. Tomasi, B. Menucci, R. Cammi, *Chem Rev* **2005**, *105,* 2999-3094.

[20] Y. Zhao, D. G. Truhlar, Theor. Chem. Acc., 2008, **120**, 215-41.

[21] C. Latouche, D. Skouteris, F. Palazzetti, V. Barone *J.* Chem. Theory Comput., **2015**, *11*, 3281-3289

[22] Z. Rinkevicius, I. Tunell, P. Sałek, O. Vahtras, H. Ågren, *J. Chem. Phys.* **2003**, *119*, 34−46.

[23] H. Ågren, O. Vahtras, B. Minaev, Adv. Quantum Chem. **1996**, *27,* 71−162.

[24] DALTON. A molecular electronic structure program. Release Dalton 2011. http://daltonprogram.org/.

[25] K. Ruud, B. Schimmelpfennig, H. Ågren, *Chem Phys Lett* **1999**, *310*, 215−21.

Entry for the Table of Contents

FULL PAPER

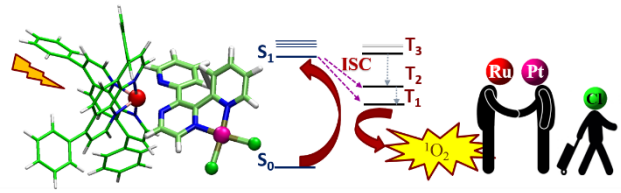

A metals' synergetic effect makes a Ru^{II}-Pt^{II} assembly promising as multitarget anticancer drug. *Cis-$PtCl_2$ moiety tunes the photophysical properties of the Ru^{II} chromophore making it suitable for PDT approach, and Ru^{II} in turn, allows for an alternative activation mechanism of Pt^{II} ligand via a ^{3}MLCT state*

Marta E. Alberto, Nino Russo, Carlo Adamo*

Page No. – Page No.

Metals' synergetic effect in a promising Ru^{II}-Pt^{II} assembly for a combined anticancer approach: Theoretical exploration of the photophysical properties